Optics and Laser Technology 101 (2018) 468–478

Contents lists available at ScienceDirect

Optics and Laser Technology

journal homepage: www.elsevier.com/locate/optlastec

Review

[INVITED] Surface plasmon cavities on optical fiber end-facets for biomolecule and ultrasound detection ☆

Tian Yang [a,*], Xiaolong He [b], Xin Zhou [a], Zeyu Lei [a], Yalin Wang [b], Jie Yang [a], De Cai [a], Sung-Liang Chen [a], Xueding Wang [c]

[a] State Key Laboratory of Advanced Optical Communication Systems and Networks, Key Laboratory for Thin Film and Microfabrication of the Ministry of Education, UM-SJTU Joint Institute, Shanghai Jiao Tong University, Shanghai 200240, China
[b] Xu Yuan Biotechnology Company, 1180 Xingxian Road, Shanghai 201815, China
[c] Department of Biomedical Engineering, University of Michigan, 2200 Bonisteel Blvd, Ann Arbor, MI 48109, USA

ARTICLE INFO

Article history:
Received 16 October 2017
Received in revised form 30 November 2017
Accepted 6 December 2017
Available online 15 December 2017

Keywords:
Lab on fiber
Optical fiber end-facet
Surface plasmon resonance
Label-free biosensing
Ultrasound detection

ABSTRACT

Integrating surface plasmon resonance (SPR) devices upon single-mode fiber (SMF) end facets renders label-free sensing systems that have a simple dip-and-read configuration, a small form factor, high compatibility with fiber-optic techniques, and invasive testing capability. Such devices are not only low cost replacement of current equipments in centralized laboratories, but also highly desirable for opening paths to new applications of label-free optical sensing technologies, such as point-of-care immunological tests and intravascular ultrasound imaging.

In this paper, we explain the requirements and challenges for such devices from the perspectives of biomolecule and ultrasound detection applications. In such a context, we review our recent work on SMF end-facet SPR cavities. This include a glue-and-strip fabrication method to transfer a nano-patterned thin gold film to the SMF end-facet with high yield, high quality and high alignment precision, the designs of distributed Bragg reflector (DBR) and distributed feedback (DFB) SPR cavities that couple efficiently with the SMF guided mode and reach quality factors of over 100, and the preliminary results for biomolecule interaction sensing and ultrasound detection. The particular advantages and potential values of these devices have been discussed, in terms of sensitivity, data reliability, reproducibility, bandwidth, etc.

Contents

1. Introduction

Integrating sensors at the ends of optical fibers, which changes the intensity, spectrum and/or phase of the fiber-guided

☆ Invited article by the Guest Editor: Yuan Gong.

* Corresponding author.
E-mail address: tianyang@sjtu.edu.cn (T. Yang).

https://doi.org/10.1016/j.optlastec.2017.12.003
0030-3992/

lightwaves upon detection of the targeted substances, is desired in a number of application scenarios, e.g., biomolecule interaction analysis, drug screening, immunological tests, agriculture produce inspection and ultrasound imaging. For they have the advantages of allowing optical access to the inside of opaque subjects, transmitting optical excitations and signals in flexible fibers and through long distances, taking advantages of the development of fiber-optic communication technologies, and providing more compact, simple and stable systems compared with the free-space optics counterparts. In addition, by placing the fiber ends right onto the targets and reading the outputs, the operation requires much less technical expertise and is much more time efficient than the alternative techniques, which is of high importance for emergent medical diagnosis, point-of-care testing (POCT), and on-site inspections.

An ideal fiber-end sensor device should satisfy the following four requirements. (1) The sensing performance, in terms of limit of detection (LOD), satisfies the targeted applications or even matches its free-space counterpart which couples to planewaves. (2) The fiber is a single-mode fiber (SMF) and the optical system is an all-fiber system. Although using a straight segment of multi-mode fiber (MMF) is an effective way to guide light into and out of the sample [1], it loses most advantages of using fiber-optics. In particular, when MMFs are applied, free-space optics setups are often involved in order to couple to the fundamental or the few lowest order fiber-guided modes, which makes the optical system complicated, bulky and incompatible with standard fiber-optic telecommunication techniques. (3) The sensor signal is collected by reflecting into and being guided through the same fiber. The end-reflection configuration is crucial for dip-and-read operation and insertion into tiny vessels. (4) Reproducibility between different devices is important for quantitative measurements and sensor arrays. This presents a challenge for device fabrication.

Despite the fact that fiber-end sensors have been investigated extensively for many years, there is limited success to achieve all of the above four requirements, which has significantly hindered progress for real applications and commercialization. In this paper, after introduction to the fabrication methods, we review our recent work on surface plasmon cavities on optical fiber end-facets for refractive index sensing, in the contexts of biomolecule detection and ultrasound detection [2–4]. In particular, we discuss the requirements on the sensor devices in further details from the application point of view, which seems to be elusive from an amount of recent device research reports. We believe these discussions are necessary to guide current device research towards producing really valuable products.

While this review focuses on fiber end-facet surface plasmon resonance (SPR) devices, reviews of a broad range of recent technical advances about lab-on-fiber nanostructures and fabrication technologies can be found in Ref. [5–9], which open many other opportunities for performance improvement and applications. In addition, there have been a number of reports on SPR devices on planar substrates whose sizes and numerical apertures match that of a SMF, which are prospective to be integrated upon SMF end-facets, e.g. SPP launching and shaping [10–14] and polarization conversion [15].

2. Device fabrication

The endeavor to fabricate nano-plasmonic structures on the tiny flat end-facets of optical fibers have been a subject under active exploration. Electron beam lithography, in spite of being the most efficient and reliable methods for patterning nanostructures on a planar substrate, becomes hugely challenging when being applied on the fiber end-facets, due to the difficulty to coat a thin layer of photoresist, the lack of a conductive substrate and the difficulty to align the nano-pattern to the core of fiber. Nonetheless, successful patterning of periodic nanodot arrays upon SMFs and concentric rings upon large core area MMFs have been successfully demonstrated [16,17]. The photoresist layers were coated by dipping the fiber tips into the resist and then shaking or blowing off the extra resist, by mounting the fiber end-facets onto flat surfaces, or by thermal evaporation [18]. Meanwhile, interference lithography has also been demonstrated, which also requires a photoresist layer [19]. On the other hand, focused ion beam milling is a much more straightforward method for fiber end-facet nano-patterning, as have been reported by several groups [20–23]. However, it is much more time consuming, and the injection of gallium ions is a severe concern for Raman spectroscopy measurements [24].

In view of the difficulties to directly pattern the fiber end-facet, a few transfer techniques have been developed in recent years, in which a nano-patterned metallic film is first fabricated on a planar substrate and then transferred to the fiber end-facet. In a nanoskiving approach, the metallic nanostructures embedded in epoxy are sectioned into thin slabs, then the slabs are floated flat on top of water and transferred to the fiber end-facets by pressing the fibers into the slabs [25]. In a decal transfer approach, the nanometallic structures are stripped from a planar substrate, and transferred to a thin sacrificial film and then the fiber end-facet in sequence [26]. This approach also enables transfer onto curved surfaces. At the same time, the transfer method proposed by Ref. [27], in which the gold nanostructures are directly stripped off silicon or SiO_2 substrates, has become a widely employed technique in nanoplasmonics device fabrication nowadays, due to the weak Van der Waals binding force between gold and the substrates, and the superior surface smoothness of the transferred gold. This transfer method has also been adopted for transferring gold nanostructures onto fiber end-facets by several groups, including us [2,28–30]. More recently, transfer by using hydrochloric acid to etch a sacrificial indium tin oxide layer has been demonstrated [31].

Fig. 1a shows the concept of our glue-and-strip fabrication approach. The details are as follows [2]. First, an amount of optical epoxy adhesive is applied on the tip of the fiber, with a careful control of the volume of the epoxy droplet. Then, the fiber is mounted on a multi-axis translation stage and moved towards the substrate which carries the gold film with the nano-patterns. The fiber is observed under a stereomicroscope and aligned with its mirror image in the gold film to be a straight line. Alignment marks on the gold film enables a coarse alignment of the fiber to the nano-pattern. Then precise alignment is achieved by sending a broadband light into the fiber, monitoring its reflection spectrum off the gold nanostructure in real-time, and optimizing the position of the fiber end. After alignment, the epoxy is either cured by a UV lamp or heating the substrate. At last, the fiber tip is moved off the substrate quickly to strip the gold film. For non-periodic nano-patterns such as a cavity, UV curing through a transparent substrate such as glass and quartz is preferred, since it avoids thermal expansion of the substrate which may severely affect the alignment. A front-view optical microscopy image of the resulting device is shown in Fig. 1b, where the irregular outer rim is the edge of the stripped and transferred thin gold film, the circular inner rim is the edge of the cladding of a bare fiber underneath the gold film, and the square-shaped shadow is a nanoslit array on the gold film. The four dark rectangles are alignment marks. In the center of the nanoslit array is an SPR cavity, which shows a lighter color than its surrounding and which is aligned to the core of fiber.

In addition, there are a plethora of other inventions to modify the fiber tips, including but not limited to the flat end-facets, e.g., direct laser writing [32–34], mechanical polishing [35–37],

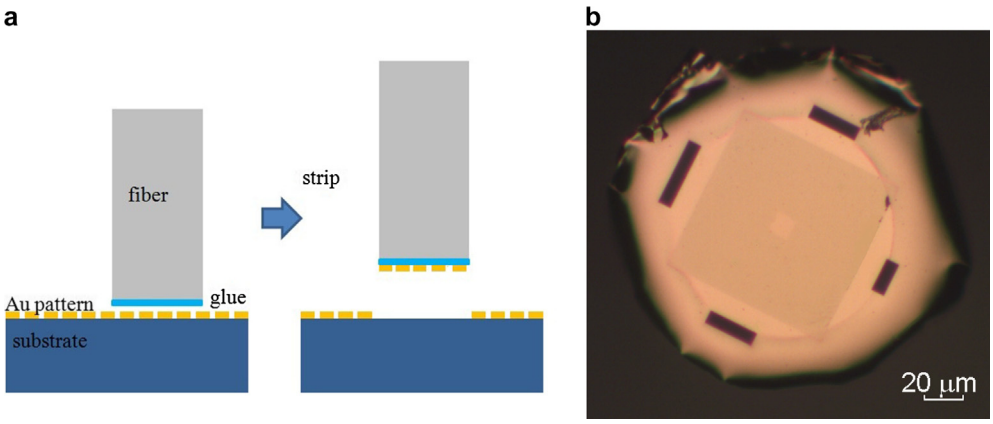

Fig. 1. Fabrication of a nano-patterned thin gold film on the end-facet of an SMF. a, The glue-and-strip process. b, The front view of the fabricated device under an optical microscope [2,29].

chemical etching and tapering [38–42], fiber-aligned photolithography [43], nanoimprinting [29], self-assembly of nanoparticles [44], and Micro-Electro-Mechanical System (MEMS) techniques [45]. A survey of these techniques can be found in Ref. [6].

3. SPR cavities on optical fiber end-facets for biomolecule sensing

3.1. Label-free biosensing: Promises, challenges and comments

Micro-optical resonators and interferometers, whose responses to external optical excitations shift with the changes in environmental refractive indices, have been widely and intensively investigated for label-free biomolecule sensing [46–48]. It has long been anticipated that the development of label-free sensing technologies, due to the fact that they significantly simply the biochemical experiments by eliminating multiple labeling steps, will revolutionize the traditional drug screening markets and bring new markets in POCT, food safety, environmental monitoring, etc., which are worth tens of billions of USDs [49–52]. In addition, SPR has been written in the pharmacopeia of the United States and Japan for the first time last year, which brings the anticipation of a fast growth of market in the near future [53]. However, more than ten years after these predictions, nowadays the applications of label-free biosensing are still mainly restricted in high-end biology laboratories and secondary drug screening in pharmacy [54,55]. The limited applications are due to the high costs and bulky sizes of the equipments, and the lengthy operation procedures which require a certain degree of professionalism. In this aspect, the successful integration of SPR at optical fiber end-facets has a great promise to fulfill the promises of label-free biosensing by providing compact, simple and fast testing equipments.

To facilitate paper writing, here we define the terminologies that have been widely adopted to characterize the performance of refractive index sensing devices, for the wavelength interrogation scenarios.

$$\text{Sensitivity}\ \ (\text{nm RIU}^{-1}) = \frac{\text{resonance wavelength shift}}{\text{refractive index increase}}, \tag{1}$$

$$\text{Figureof merit, FOM}\ \ (\text{RIU}^{-1}) = \frac{\text{Sensitivity}}{\text{FWHM linewidth of resonance spectrum}}, \tag{2}$$

$$\text{Limit of detection, LOD}\ \ (\text{RIU}) = \frac{3 \times \text{RMS noise of resonance wavelength}}{\text{Sensitivity}}. \tag{3}$$

It seems that many optical physicists' efforts in this field have been contributed to improve the sensitivity and LOD, with the ultimate goal of single molecule detection. However, the following points should be noted with regard to this aspect. (1) The minimum amount of molecules that can be detected is not only dependent upon LOD, but also upon a number of other important factors. For a well-designed system, the root-mean-square (RMS) noise after being averaged for around a second is typically smaller than the baseline drift in a few minutes. The baseline drift not only comes from the system but also the instability of the chemically functionalized sensor surface. Further, non-specific binding often overwhelms the noise and baseline drifts, especially in complicated samples such as blood and urine, in which situations the mass of analytes adsorbed on the sensor surface should be improved rather than the LOD. (2) For quantitative analysis, the minimum amount of molecules that can be detected should be defined together with the variance between different tests performed on different days using different sensors. For example, in the case of high-sensitivity cardiac troponin (hs-cTn) tests for clinical diagnosis of myocardial infarction, the coefficient of variance is required to be within 10% for each assay at the 99th percentile for a reference control group, according to the Joint European Society of Cardiology/American College of Cardiology Committee [56]. (3) The minimum amount of molecules that can be detected is significantly affected by the diffusion of molecules. To ensure a fast enough mass transfer in the sample solution so as to maintain the concentration of analyte molecules near the sensor surface, the samples are flowed or stirred at fast speeds in commercial equipments [1,57,58]. However, this brings a fundamental difficulty to localized surface plasmon resonance (LSPR) devices, in which mass transfer into the local hotspots is both difficult and at different speeds for different "corners" of the nanostructures. Consequently, the combination of different mass transfer speeds in the same sample makes the biomolecule interaction sensorgram deviate from a simple exponential curve, as can be observed in published data but rarely noted. (4) Intrinsically, it is difficult for label-free sensing technologies to compete with the mature labeling technologies, such as fluorescence and chemiluminescence, with regard to LOD. The inherent advantage of label-free biosensing is, instead, the capability to monitor biomolecule interactions in real-time, and in a fast and convenient way. Therefore, simple operation and a compact system shall not be sacrificed for achieving low LOD, if we target the tremendous applications beyond high-end laboratories. (5) At last, to claim the detection of a very low concentration of molecules, a reference test with no specific receptors on the sensor surface must be conducted for comparison, which is surprisingly often missing from optical device research

papers. In fact, a quick comparison between a number of research papers and the Biacore product datasheet will indicate that the FOMs and the baseline drifts of the former are far from enough to support the conclusion of detecting the claimed ultralow concentration. Non-specific binding, water stains and substances from the walls of containers can all possibly be what had been actually detected in these research papers.

3.2. SPR cavities on single-mode fiber end-facets

In the well-known Kretschmann configuration for SPR prism coupling, the illumination is at an incident angle larger than the critical angle for total internal reflection (TIR), which can be readily incorporated by fiber side-wall SPR devices. The fiber side-wall devices have taken the configurations of exposed fiber cores, chemically etched tapers, long-period grating coupling, titled Bragg grating coupling, etc. [5,7,8,47,59–72].

However, the design of SPR structures on optical fiber end-facets can't straightforwardly inherit their free-space optics counterparts. The Q values and coupling efficiencies of most grating-coupled SPR structures for planewave coupling at normal incidence, when coupled to the fiber in the end-fire configuration, degrade significantly. This is due to the fact that these structures consist of a periodic array of nanostructures in a metallic film, while the fiber-guided lightwaves have a finite numerical aperture (NA). This effect can be understood from two perspectives [2]. Firstly, when the periodic grating is illuminated by the fiber-guided lightwaves at normal incidence, it is equivalent to grating coupling of a superposition of planewaves with different angles of incidence within the NA. Since the grating-coupled SPR's resonance wavelength shifts with the incidence angle of planewave, the superposition broadens the SPR spectrum and reduces the coupling efficiency at a single wavelength. Secondly, let's assume a virtual SPR mode which has a transverse modal area that matches the fiber-guided lightwaves. A fundamental difference between this SPR mode - fiber-guided mode coupling system and the SPR – planewave coupling system is that the former contains an extra SPR modal loss which is surface plasmon polariton (SPP) propagation out of the modal area. This extra loss term item is so significant for the small core area of a SMF that it severely broadens the SPR spectrum and moves the system far away from critical coupling. To date, there have been a variety of periodic nanoplasmonic structures fabricated on the end-facets of SMFs and MMFs, including nanoholes, nanoparticles, nanoslits and gratings [5,8,9,16,19–26,29,30,44,73–76]. Many of these devices were used to demonstrate surface enhanced Raman spectroscopy (SERS) instead of refractive index sensing due to the broad linewidths of the SPR spectra.

According to the abovementioned second perspective, in order to improve the Q and spectral depth of SPR at the fiber end-facet, it is critical to mitigate the SPP propagation out of the modal area. Therefore, forming a cavity to confine the SPPs is a reasonable solution. Recently, two cavity designs have been demonstrated by us, one using a distributed Bragg reflector (DBR) to confine the SPP mode in the SPP band [2], the other using a phase shift section in a second-order distributed-feedback (DFB) grating to create a defect mode in the SPP bandgap [3]. Both show a high Q SPR, a greatly improved FOM compared to previous work, and a LOD on the order of 10^{-6} RIU.

In the following, we briefly summarize the design and characterization of our SPR cavity devices on SMF end-facets. The front view of one of the first type of devices under an optical microscope has been shown in Fig. 1b. In this device, a 55 nm thick gold film covers the end-facet of a SMF. The square shadow is an array of 50 nm wide nanoslits penetrating through the gold film. The slits in the central lighter color region have a period, Λ_1, of 645 nm, and occupy an area of around $11 \times 1\ \mu m^2$. The slits in the surrounding region have a period, Λ_2, of 315 nm. A scanning electron micrograph (SEM) image around the interface between the central and surrounding slit regions is shown in Fig. 2a. The square design makes the device performance insensitive to the polarization of the fiber-guided lightwaves. A 2-D schematic illustration of the device is shown in Fig. 2b, where the fiber has been simplified into a 2-D dielectric waveguide with the same core diameter and refractive indices as a standard SMF.

The central nanoslit array couples the fiber-guided lightwaves and the SPPs through its first order spatial Fourier component, same as commonly used grating-coupled SPR for planewave coupling. In addition, it also has a considerable second-order spatial Fourier component due to the tiny width of the slits, which results in bandgaps in the SPP band diagram. The SPP band diagram of the central 2-D structure in Fig. 2b, which is taken to be infinitely extended in the in-plane direction, has been calculated by finite-difference time-domain (FDTD) calculation, and plotted in Fig. 3. Here, the power reflectivity for *p*-polarized planewaves incident within a range of wavelengths and in-plane wave-vectors is plotted. In the figure, the points A and B correspond to SPPs on the water-gold interface, and C and D correspond to SPPs on the (fiber) glass-gold interface. A and C are bright modes under normally incident illumination, and B and D are dark modes which only show up under tilted illumination. A is the SPR mode that we use for detecting molecules in the water.

The surrounding nanoslit array forms a DBR to confine SPPs in the cavity. The distance between the two nanoslit arrays, *s*, is designed to achieve constructive interference between the two

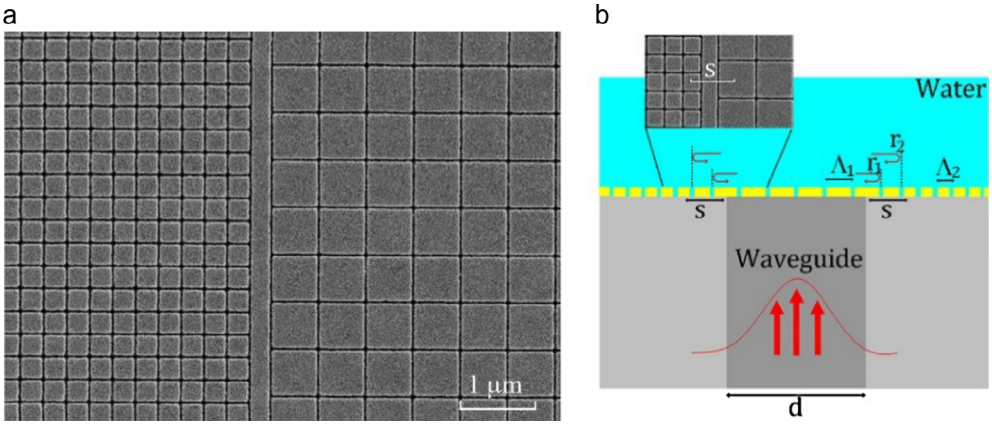

Fig. 2. The DBR SPP cavity. a, The SEM image of the interface between the central and surrounding nanoslit arrays. b, A 2-D schematic illustration of the device, in which the gold film is in yellow [2]. (For interpretation of the references to colour in this figure legend, the reader is referred to the web version of this article.)

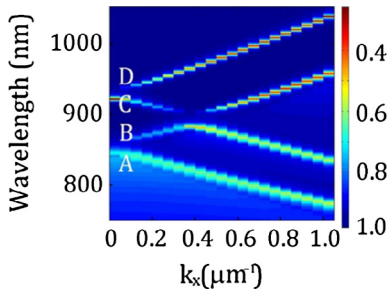

Fig. 3. The SPP band diagram of the 2-D central nanoslit array calculated by FDTD [2].

reflections at the interface, which are labeled as r_1 and r_2 in Fig. 2b.

The second type of devices' SEM image and 2-D schematic illustration are shown in Fig. 4. The same nanoslit array in a thin gold film is used to grating-couple the fiber-guided lightwaves to SPPs along the water-gold interface. Borrowing the concept of DFB laser cavity, a phase-shift section with a length of s is inserted in the center of the cavity to create a defect SPP mode.

The SPP band diagram of the 2-D periodic nanoslit array is shown in Fig. 5a, together with the light lines of water and glass. Here, it has been calculated by using pulsed dipole sources to excite the SPP fields, and performing Fourier transform on the time-domain fields to find the frequencies of the SPP modes under the Bloch boundary condition for each in-plane wave-vector k_x. The coupling between a normally incident p-polarized illumination and the SPPs along the gold-water interface corresponds to the $k_x = 0$ point on the shortest wavelength band, coupled by the first order spatial Fourier component of the nanoslit array. Meanwhile, the same as in the first type of devices, the strong second-order spatial Fourier component of the nanoslit array produces a bandgap from 865 nm to 877 nm, as indicated by the blue dash-dot lines. In Fig. 5b, the p-wave power reflectivity of the 2-D waveguide upon the 2-D nanoslit array as in Fig. 4b has been calculated by FDTD and plotted. It shows that by inserting the phase-shift section, a defect mode appears within the bandgap, whose wavelength shifts with s and moves out of the bandgap and cycles when s is further increased. It is noteworthy that a set of odd symmetry defect modes are not excited in the calculation and not shown in Fig. 5b.

In Fig. 6, the electric field intensity distributions of the 2-D SPR field without and with a phase-shift section $s = 110$ nm are compared, at 850 and 871 nm, respectively. The on-band mode extends in-plane until it extinguishes by ohmic and scattering losses, while the defect mode is confined near the core of waveguide due to forbidden propagation in the DFB structure.

The experimental setup to characterize the sensors is schematically illustrated in Fig. 7. The fiber is a typical SMF for 780 nm. A super-luminescent diode (SLD) is used as the light source. A

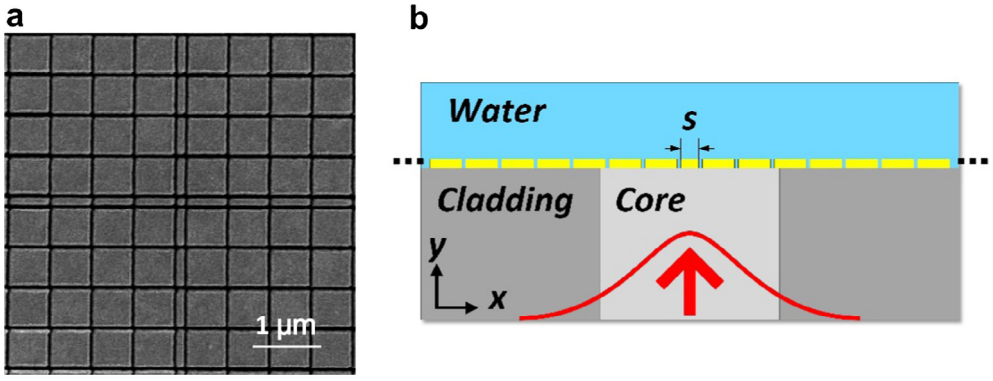

Fig. 4. The DFB SPP cavity. a, The SEM image of the center of the device. b, A 2-D schematic illustration of the device, in which the gold film is in yellow [3]. (For interpretation of the references to color in this figure legend, the reader is referred to the web version of this article.)

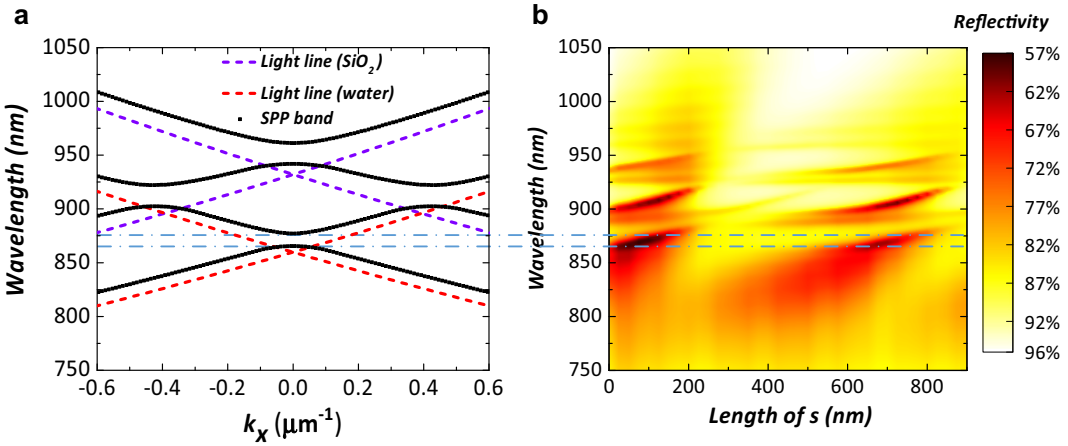

Fig. 5. The SPP band diagram of the 2-D DFB cavity calculated by FDTD. a, A periodic nanoslit array. b, With a phase shift section of length s [3].

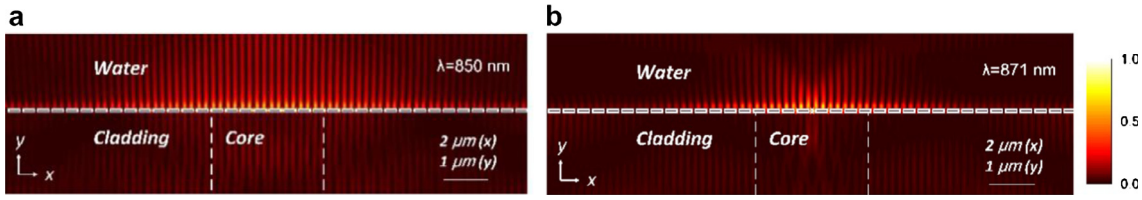

Fig. 6. The 2-D electric field intensity distributions of the SPR fields under waveguide illumination. a, A periodic nanoslit array. b, With a phase shift section of length s = 110 nm [3].

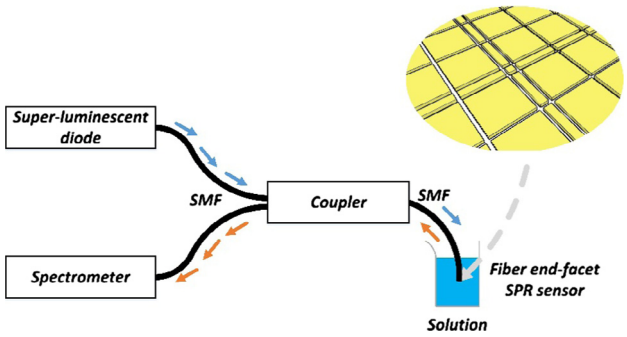

Fig. 7. The biosensing experiment setup [3].

50–50% fiber directional coupler routes the fiber-guided light-waves to the SPR sensor probe. Reflection off the sensor is routed to a fiber-coupled CCD spectrometer. It is important that a fiber-coupled SLD is used as the light source, since it sends enough optical power into the SMF in order to achieve a high signal-to-noise ratio (SNR). This is impossible when the SPR Q is low and a broader band light source such as a halogen lamp has to be used to cover all of the SPR spectral range. Such lamps couple extremely inefficiently into an SMF, which results in a much lower SNR.

The normalized reflection spectra when an SPR sensor of the first type is immersed in seven different liquids are shown in Fig. 8, together with a plot of SPR central wavelength versus refractive index. The Q values are around 101, and the SPR spectral dips' depths are around 20%. A good linearity within a broad range of refractive indices is observed, with a sensitivity of 571 nm RIU^{-1}. The FOM is determined to be 68 RIU^{-1}, showing over an order of magnitude improvement to previous reports on SMF end-facet periodic SPR structures. The LOD is measured to be 3.5×10^{-6} RIU with a 1 s integration time, showing two orders of magnitude improvement to previous reports on optical fiber end-facet SPR sensors. A sensor of the second type has been measured to have a sensitivity of 628 nm RIU^{-1} and a FOM of 80 RIU^{-1}. We expect that with more nanoplasmonic structures being designed and mechanisms being understood, the sensing performance will have a large space to be further improved in the future.

In Fig. 9, the result of a real-time biosensing experiment using our fiber end-facet SPR cavity sensor is shown. Here, 1 RU corresponds to approximately 1 pg mm^{-2} surface mass density of adsorbed molecules. In the experiment, first the sensor with a bare gold surface is immersed in a 4-(2-hydroxyethyl)-1-piperazineetha nesulfonic acid (HEPES) buffer solution to obtain a baseline. Then the sensor is immersed in a (poly-L-lysine)-(polyethylene glycol)-biotin (PPB) solution to form an antifouling layer by electrostatic forces, in order to reduce the nonspecific binding [77,78]. Next, a layer of streptavidin (SA) is added on top of the PPB through biotin-SA binding. Then, a layer of biotinylated protein A (BPA) is added on top through SA-biotin binding. Finally, the sensor with a protein A surface is used to capture human immunoglobulin G molecules. In each step, after binding with the target molecules, the sensor is immersed in HEPES to wash off extra molecules or to observe the dissociation process. The switching to HEPES time moments are labeled by arrows in the figure.

4. SPR cavities on optical fiber end-facets for ultrasound detection

To achieve high resolution and fast speed ultrasound imaging, it is desired that the ultrasound detection technique has a low noise equivalent pressure (NEP), a broad band frequency response, a broad angular response and the ability to perform phased-array detection. In addition, for invasive applications, e.g., intravascular imaging, ultra-compact sensor probes and signal transmission cables are necessary, in which situation the fiber-end devices have

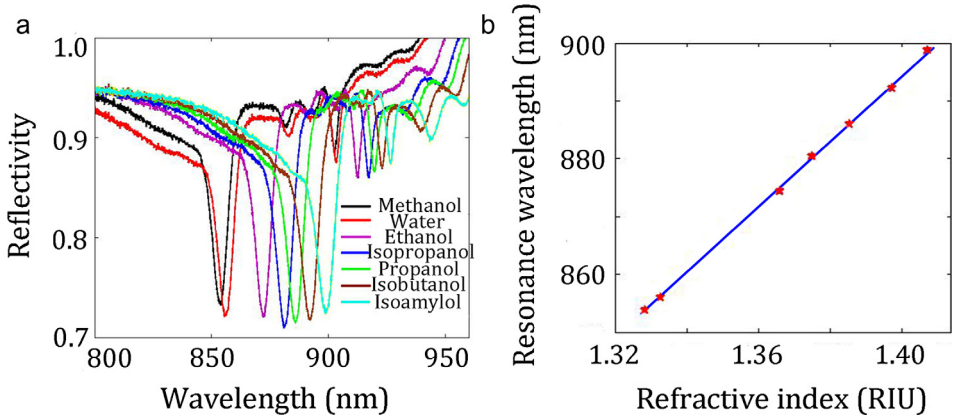

Fig. 8. Refractive index sensing experiment results. a, SPR spectra for different solutions. b, SPR resonance wavelength versus refractive index [2].

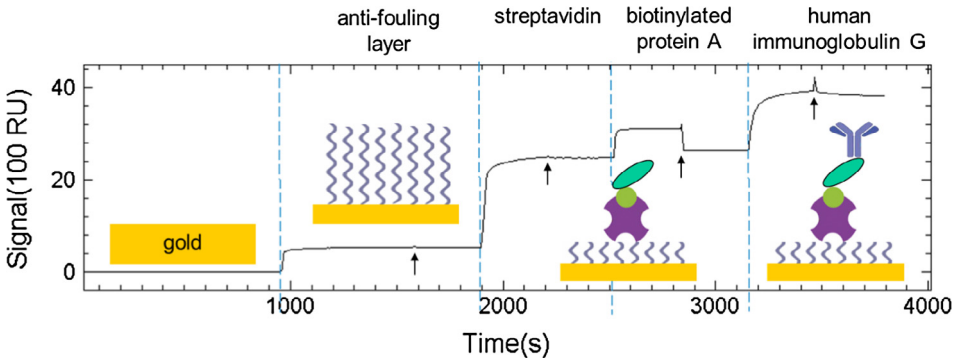

Fig. 9. Biomolecule interaction monitoring experiment results.

obvious advantages. In particular, SMF should be applied when the fiber cable is constantly moving in the *in vivo* environment.

For traditional piezoelectric hydrophones, there is a compromise between NEP and bandwidth/angular response. The sensitivity increases with the size of the sensing element by harvesting more acoustic waves. On the other hand, the acoustic pressures in the sensing element cancel each other when they are out of phase, i.e., when piezzoelectric material dimension $\geqslant \frac{1}{2}\frac{\text{acoustic wavelength}}{\cos\theta_i}$, where θ_i is the incident angle of the ultrasound wave.

In the last twenty years or so, there have been quite a number of research work on acousto-optical micro-devices for ultrasound detection [4,79–89]. The fundamental signal transduction principle is detecting the change in refractive index and/or device morphology under acoustic pressure, which results in a shift in the micro-resonator's resonance wavelength and a consequent change in the reflectivity or transmissivity of a fixed-wavelength laser. Due to the ultrahigh Q values and the micrometer scale thicknesses of the optical resonant modes, the latest NEP and bandwidth values reported are as good as on the order of Pa $MHz^{-1/2}$ and 100 MHz, respectively [81,85,87,88]. Among them, Fabry-Pérot (F-P) cavities have been fabricated on the SMF end-facets [82–85]. An NEP of 5 kPa over a 20 MHz bandwidth and a bandwidth of 50 MHz have been reported for a flat mirror F-P cavity in 2009, and the device has been implemented in the commercial UMS3 scanning system of Precision Acoustics [82]. More recently, NEP values as low as 4 Pa over 5 MHz [85] have been reported, by creating spherical mirrors under surface tension.

The SPR cavity sensors on SMF end-facets as described in Section 3 are also good candidates for ultrasound detection. They have two advantages over the dielectric resonators as follows. First, the active volume for sensing is ultra-small, which has a transverse area comparable to the SMF guided optical mode, and an evanescent depth equal to that of the SPPs. Therefore, a large bandwidth for a wide angular range of detection is in principle possible. Second, different from the dielectric resonators, in which the acoustic sensitive material has to be the wave-guiding material at the same time, in our devices we can choose the overlaying layer from a wide range of highly acoustic sensitive materials and nanostructures to cover the evanescent SPP field. It is noteworthy that pursuing high Q values, as in previous work, will risk the reproducibility between different devices which is critical for phased array, while pursuing highly acoustic sensitive overlaying layers with intermediate Q values may be a more viable solution in this situation.

Fig. 10 is a picture of our ultrasound sensor packaged in a fiber-optic cable ferrule, which contains a ceramic rod and a metallic housing [4]. The SPR cavity sits at the end-facet of a bare optical

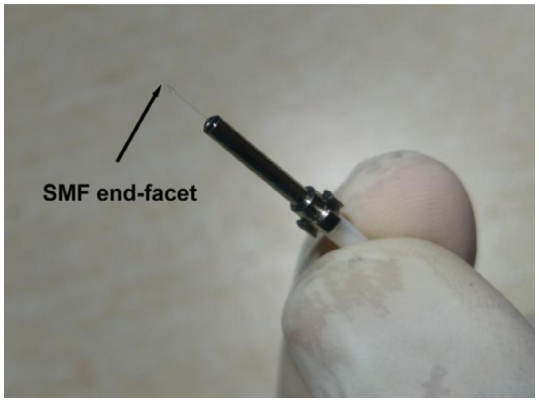

Fig. 10. The sensor probe packaged in a fiber-optic cable ferrule [4].

fiber that protrudes out of the metallic housing for about 10 mm. The device design concept and fabrication method inherit our work on the first type of biomolecule sensing devices as described in Section 3, and will not be repeated. Here, Λ_1 is 1020 nm, Λ_2 is 504 nm, and s is 500 nm. The SMF guided lightwaves around 1550 nm are coupled to SPPs on the gold-epoxy interface, though the SPPs on the gold-water interface can be used as well [86].

Fig. 11a is a schematic illustration of our ultrasound measurement system, where a tunable laser's output is guided by the SMF to the SPR cavity, interacts with the ultrasound signal, and is received by a photodetector and an oscilloscope. Fig. 11b shows the experimental SPR spectrum, which has a Q of 282 and a resonance dip depth of 45%. Theoretically, the refractive index sensitivity is 876 nm RIU^{-1} within a large range of refractive indices. The tunable laser wavelength is set at either side of the SPR dip to measure the ultrasound output of a piezoelectric transducer. The reflected laser power versus time is plotted in Fig. 4c and d at 1539 nm and 1543 nm, respectively. The opposite polarities of the two measurement results are due to the opposite signs of the SPR dip slopes [4].

By calibrating our sensing system using the UMS3 system [4], we have obtained an NEP of 5.2 kPa over 20 MHz, a 6 dB angle of 70° at 10 MHz, and a stable performance for 20 min in ambient conditions without feedback control. By using a pulsed laser with a 5 ns pulse duration and a 532 nm wavelength to pump a 200 nm thick chromium film, we have generated short ultrasound pulses and calibrated our sensor's bandwidth to be over 125 MHz, which is limited by our measurement method. We expect the sensitivity of our sensors to be significantly improved in future work by applying acoustic sensitive materials and metamaterials that have much smaller elastic moduli as the overlaying layer.

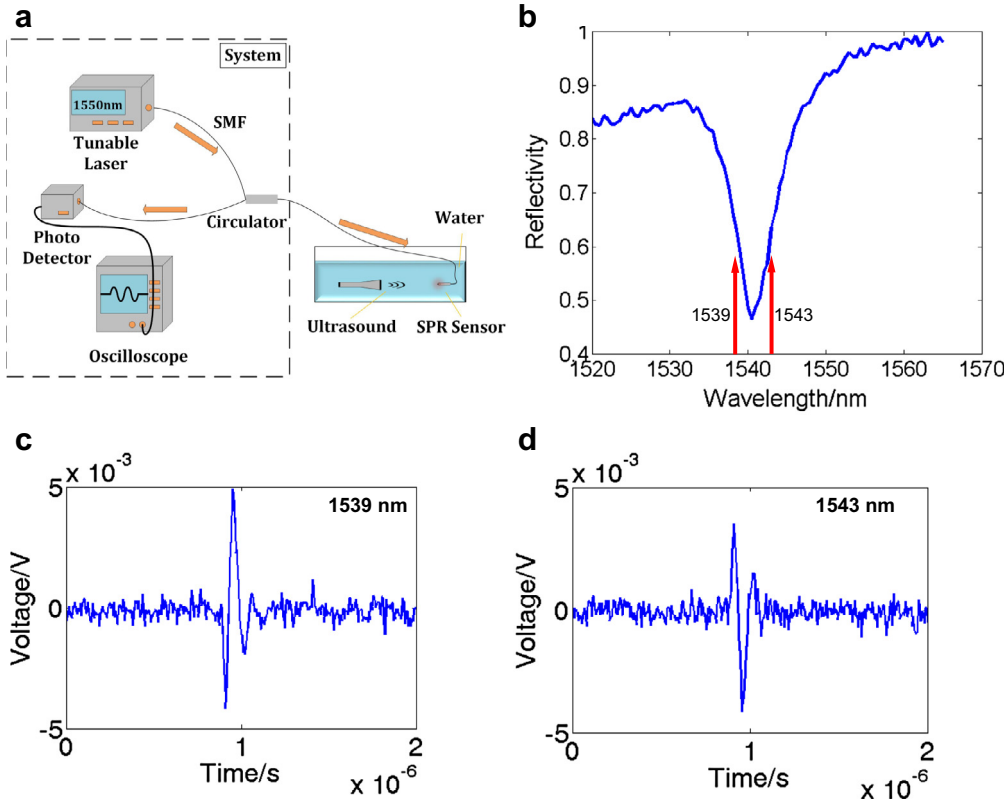

Fig. 11. Ultrasound detection experiment. a, The experiment setup. b, The SPR spectrum. c & d, The oscilloscope readouts of the same ultrasound pulses, by setting the laser wavelength at the opposite sides of the SPR dip [4].

5. Conclusion

We have discussed the advantages and potentials of refractive index sensors integrated at optical fiber end-facets, particularly for biomolecule and ultrasound detection applications. Specific requirements and challenges from the application point of view have been elaborated, including comments on how to correctly evaluate the device performance and pursue their potential values.

A review of our recent work on SMF end-facet SPR cavities has been conducted in the above context, together with a brief introduction to the other fabrication techniques and devices developed in the field. In our work, using a glue-and-strip fabrication technique, nano-patterned gold films are transferred from a planar substrate to the fiber end-facet with high quality and with high alignment precision to the fiber core. By either confining an SPR mode on the SPP band with a DBR, or creating a defect SPR mode in the second-order DFB bandgap, the SMF excided SPPs are in the form of a cavity mode that spatially matches the fiber-guided lightwave mode. The resulting SPR resonances show Q values around 100 and sensitivity values up to 628 nm RIU^{-1} near 850 nm, and a Q of 282 and a sensitivity of 876 nm RIU^{-1} near 1550 nm.

For biomolecule detection, we believe the values and/or potentials of fiber end-facet label-free sensors are fast and convenient operations, compact systems and invasive detection. At the same time, a reasonable LOD should be reached in the context that there are other highly sensitive labeling technologies available. A good reproducibility between different devices must be satisfied as well. The LOD of our sensors with an SLD light source is on the order of 10^{-6} RIU at 1 s integration time. A real-time biomolecule interaction sensorgram has been shown, which outperforms a MMF-based commercial equipment (comparison data not shown).

For ultrasound detection, the particular advantages of our SPR cavity sensors include an ultrasmall acoustic sensing volume which allows large bandwidth and wide angle detection, the freedom to apply highly acoustic sensitive materials and nanostructures to interact with the SPP field (in future work), and the reproducibility between different devices which is critical for phased arrays.

As the performance of SMF end-facet SPR sensors continue to improve, not only will they replace some of the expensive and bulky equipments in high-end laboratories, but more importantly it holds out the prospect to fulfill the long-time expectation to have label-free sensing technologies find tremendous values in new application areas, including immunological diagnosis, medical imaging, high throughput drug screening, food safety, etc.

Funding

This work was supported by the National Science Foundation of China [grant # 61275168 and 11574207], the National High Technology R&D Program of China [grant # 2015AA020944], the Xu Yuan Biotechnology Co. and the Shanghai Jiao Tong University Med-Eng X program.

Acknowledgement

We thank Prof. Xuexin Duan and Ziyu Han from Tianjin University for providing the PPB molecules. We thank Prof. Aili Zhang and Ying Xin from Shanghai Jiao Tong University, and Prof. Qian Cheng, Hao Chen and Yudi Chen from Tongji University for the use of their equipments and technical assistance. Nano-fabrication has been done at the Center for Advanced

Electronic Materials and Devices of Shanghai Jiao Tong University. The biomolecule interaction sensorgram has been obtained with Xu Yuan Biotechnology Company's prototype equipment.

References

[1] <https://www.fortebio.com>.
[2] X. He, H. Yi, J. Long, X. Zhou, J. Yang, T. Yang, Plasmonic crystal cavity on single-mode optical fiber end facet for label-free biosensing, Appl. Phys. Lett. 108 (23) (2016) 231105.
[3] Z. Lei, X. Zhou, J. Yang, X. He, Y. Wang, T. Yang, Second-order distributed-feedback surface plasmon resonator for single-mode fiber end-facet biosensing, Appl. Phys. Lett. 110 (17) (2017) 171107.
[4] X. Zhou, D. Cai, X. He, S. L. Chen, X. Wang, Tian Yang, Ultrasound Detection with Surface Plasmon Resonance on Fiber End-facet, in: Conference on Lasers and Electro-Optics, OSA Technical Digest, paper SM1C.3, 2017.
[5] G.F.S. Andrade, A.G. Brolo, Nanoplasmonic structures in optical fibers, in: A. Dmitriev (Ed.), Nanoplasmonic Sensors, Springer, 2012, pp. 290 (Chapter 12).
[6] G. Kostovski, P.R. Stoddart, A. Mitchell, The optical fiber tip: an inherently light-coupled microscopic platform for micro- and nanotechnologies, Adv. Mater. 26 (23) (2014) 3798–3820.
[7] C. Caucheteur, T. Guo, J. Albert, Review of plasmonic fiber optic biochemical sensors: improving the limit of detection, Anal. Bioanal. Chem. 407 (14) (2015) 3883–3897.
[8] P. Vaiano, B. Carotenuto, M. Pisco, A. Ricciardi, G. Quero, M. Consales, A. Crescitelli, E. Esposito, A. Cusano, Lab on Fiber Technology for biological sensing applications, Laser Photon. Rev. 10 (6) (2016) 922–961.
[9] F. Liu, X. Zhang, Sensors based on metallic photonic structures integrated onto end facets of fibers, Laser & Optoelectronics Progress 54(2) (2017) 020001-01-020001-11.
[10] D. Wang, T. Yang, K.B. Crozier, Optical antennas integrated with concentric ring gratings: electric field enhancement and directional radiation, Opt. Express 19 (3) (2011) 2148–2157.
[11] B. Liu, D. Wang, C. Shi, K.B. Crozier, T. Yang, Vertical optical antennas integrated with spiral ring gratings for large local electric field enhancement and directional radiation, Opt. Express 19 (11) (2011) 10049–10056.
[12] A. Baron, E. Devaux, J.C. Rodier, J.P. Hugonin, E. Rousseau, C. Genet, T.W. Ebbesen, P. Lalanne, Compact antenna for efficient and unidirectional launching and decoupling of surface plasmons, Nano Lett. 11 (10) (2011) 4207–4212.
[13] A. Pors, M.G. Nielsen, T. Bernardin, J.-C. Weeber, S.I. Bozhevolnyi, Efficient unidirectional polarization-controlled excitation of surface plasmon polaritons, Light: Sci. Appl. 3(8) (2014) e197.
[14] Z. Lei, T. Yang, Gap plasmon resonator arrays for unidirectional launching and shaping of surface plasmon polaritons, Appl. Phys. Lett. 108 (16) (2016) 161105.
[15] Z. Lei, T. Yang, Converting state of polarization with a miniaturized metasurface device, IEEE Photon. Technol. Lett. 29 (7) (2017) 615–618.
[16] Y. Lin, Y. Zou, Y. Mo, J. Guo, R.G. Lindquist, E-Beam patterned gold nanodot arrays on optical fiber tips for localized surface plasmon resonance biochemical sensing, Sensors 10 (10) (2010) 9397–9406.
[17] S. Feng, S. Darmawi, T. Henning, P.J. Klar, X. Zhang, A miniaturized sensor consisting of concentric metallic nanorings on the end facet of an optical fiber, Small 8 (12) (2012) 1937–1944.
[18] J. Zhang, C. Con, B. Cui, Electron beam lithography on irregular surfaces using an evaporated resist, Acs Nano 8 (4) (2014) 3483–3489.
[19] S. Feng, X. Zhang, H. Wang, M. Xin, Z. Lu, Fiber coupled waveguide grating structures, Appl. Phys. Lett. 96 (13) (2010) 133101.
[20] A. Dhawan, J.F. Muth, D.N. Leonard, M.D. Gerhold, J. Gleeson, T. Vo-Dinh, P.E. Russell, FIB fabrication of metallic nanostructures on end-faces of optical fibers for chemical sensing applications, J. Vac. Sci. Technol. B 26 (6) (2008) 2168–2173.
[21] H. Nguyen, F. Sidiroglou, S.F. Collins, T.J. Davis, A. Roberts, G.W. Baxter, A localized surface plasmon resonance-based optical fiber sensor with sub-wavelength apertures, Appl. Phys. Lett. 103 (19) (2013) 193116.
[22] G.F.S. Andrade, J.G. Hayashi, M.M. Rahman, W.J. Salcedo, C.M.B. Cordeiro, A.G. Brolo, Surface-enhanced resonance raman scattering (SERRS) using Au nanohole arrays on optical fiber tips, Plasmonics 8 (2) (2013) 1113–1121.
[23] A. Micco, A. Ricciardi, M. Pisco, V. La Ferrara, A. Cusano, Optical fiber tip templating using direct focused ion beam milling, Sci. Rep. 5 (2015) 15935.
[24] E.J. Smythe, M.D. Dickey, J. Bao, G.M. Whitesides, F. Capasso, Optical antenna arrays on a fiber facet for in situ surface-enhanced Raman scattering detection, Nano Lett. 9 (3) (2009) 1132–1138.
[25] D.J. Lipomi, R.V. Martinez, M.A. Kats, S.H. Kang, P. Kim, J. Aizenberg, F. Capasso, G.M. Whitesides, Patterning the tips of optical fibers with metallic nanostructures using nanoskiving, Nano Lett. 11 (2) (2011) 632–636.
[26] E.J. Smythe, M.D. Dickey, G.M. Whitesides, F. Capasso, A technique to transfer metallic nanoscale patterns to small and non-planar surfaces, Acs Nano 3 (1) (2009) 59–65.
[27] P. Nagpal, N.C. Lindquist, S.-H. Oh, D.J. Norris, Ultrasmooth patterned metals for plasmonics and metamaterials, Science 325 (5940) (2009) 594–597.
[28] S. Scheerlinck, D. Taillaert, D. Van Thourhout, R. Baets, Flexible metal grating based optical fiber probe for photonic integrated circuits, Appl. Phys. Lett. 92 (3) (2008) 031104.
[29] X. He, J. Long, H. Yi, L. Chen, Y. Tang, T. Yang, Transferring planar surface plasmon resonance structures onto fiber end facets and integration with microfluidics, in: Frontiers in Optics, Technical Digest, paper FTu1B.1, 2013.
[30] P. Jia, J. Yang, Integration of large-area metallic nanohole arrays with multimode optical fibers for surface plasmon resonance sensing, Appl. Phys. Lett. 102 (24) (2013) 243107.
[31] X. Zhang, F. Liu, Y. Lin, Direct transfer of metallic photonic structures onto end facets of optical fibers, Front. Phys. 4 (2016).
[32] Z. Ran, Y. Rao, J. Zhang, Z. Liu, B. Xu, A miniature fiber-optic refractive-index sensor based on laser-machined fabry perot interferometer tip, J. Lightwave Technol. 27 (23) (2009) 5426–5429.
[33] H.E. Williams, D.J. Freppon, S.M. Kuebler, R.C. Rumpf, M.A. Melino, Fabrication of three-dimensional micro-photonic structures on the tip of optical fibers using SU-8, Opt. Express 19 (23) (2011) 22910–22922.
[34] Z. Xie, S. Feng, P. Wang, L. Zhang, X. Ren, L. Cui, T. Zhai, J. Chen, Y. Wang, X. Wang, W. Sun, J. Ye, P. Han, P.J. Klar, Y. Zhang, Demonstration of a 3D radar-like SERS sensor micro- and nanofabricated on an optical fiber, Adv. Opt. Mater. 3 (9) (2015) 1232–1239.
[35] Y.C. Kim, W. Peng, S. Banerji, K.S. Booksh, Tapered fiber optic surface plasmon resonance sensor for analyses of vapor and liquid phases, Opt. Lett. 30 (17) (2005) 2218–2220.
[36] S. Yakunin, J. Heitz, Microgrinding of lensed fibers by means of a scanning-probe microscope setup, Appl. Opt. 48 (32) (2009) 6172–6177.
[37] Y.A. Gharbia, Special purpose nano-grinding machine for fabrication of different profiles on optical fibers endfaces, Asian Trans. Eng. 1 (2012) 1–9.
[38] P. Hoffmann, B. Dutoit, R.P. Salathe, Comparison of mechanically drawn and protection layer chemically etched optical fiber tips, Ultramicroscopy 61 (1–4) (1995) 165–170.
[39] S.I. Hosain, Y. Lacroute, J.P. Goudonnet, A simple low-cost highly reproducible method of fabricating optical fiber tips for a photon scanning tunneling microscope, Microwave Opt. Technol. Lett. 13 (5) (1996) 243–248.
[40] P.K. Wong, T.H. Wang, C.M. Ho, Optical Fiber Tip Fabricated by Surface Tension Controlled Etching, Proc. of Solid-State Sensor, Actuator and Microsystems Workshop, 2002, pp. 06269–12157.
[41] Y.J. Chang, Y.C. Chen, H.L. Kuo, P.K. Wei, Nanofiber optic sensor based on the excitation of surface plasmon wave near fiber tip, J. Biomed. Opt. 11 (1) (2006) 014032.
[42] Y.H. Tai, P.K. Wei, Sensitive liquid refractive index sensors using tapered optical fiber tips, Opt. Lett. 35 (7) (2010) 944–946.
[43] A. Petrušis, J.H. Rector, K. Smith, S. de Man, D. Iannuzzi, The align-and-shine technique for series production of photolithography patterns on optical fibres, J. Micromech. Microeng. 19 (4) (2009) 014032.
[44] M. Pisco, F. Galeotti, G. Quero, A. Iadicicco, M. Giordano, A. Cusano, Miniaturized sensing probes based on metallic dielectric crystals self-assembled on optical fiber tips, Acs Photon. 1 (10) (2014) 917–927.
[45] D. Iannuzzi, S. Deladi, J.W. Berenschot, S. de Man, K. Heeck, M.C. Elwenspoek, Fiber-top atomic force microscope, Rev. Sci. Instrum. 77 (10) (2006) 106105.
[46] J. Homola, S.S. Yee, G. Gauglitz, Surface plasmon resonance sensors: review, Sens. Actuat. B-Chem. 54 (1–2) (1999) 3–15.
[47] X. Fan, I.M. White, S.I. Shopova, H. Zhu, J.D. Suter, Y. Sun, Sensitive optical biosensors for unlabeled targets: a review, Anal. Chim. Acta 620 (1–2) (2008) 8–26.
[48] B. Špačková, P. Wrobel, M. Bockova, J. Homola, Optical biosensors based on plasmonic nanostructures: a review, Proc. IEEE 104 (12) (2016) 2380–2408.
[49] J. Comley, Label-Free Detection: New Biosensors Facilitate Broader Range of Drug Discovery Applications, Drug Discovery World, Winter, 2004.
[50] A European roadmap for photonics and nanotechnologies, the Merging Optics & Nanotechnologies (MONA) consortium, 2008.
[51] B. Roussel, J. Cochard, C. Bouye, Biophotonics Market: Technologies and Market Analysis, European Photonics Industry Consortium, Tematys and Yole Développement, 2013.
[52] Label-Free Binding Analysis Trends, HTStec Ltd., 2014.
[53] The United States Pharmacopeia, Thirty-Ninth Revision, <1105> Immunological test methods – surface plasmon resonance, pp. 1272–1288.
[54] Label Free Detection Market By Technology, By Product Type, By Application, And By Region – Global Industry Analysis, Size, Share, Growth, Trends, And Forecasts (2016–2021), Market Data Forecast, 2017.
[55] Label-Free Detection Market by Technology, Products, Applications, End User - Global Forecast to 2022, MarketsandMarkets, 2017.
[56] The Joint European Society of Cardiology/American College of, Cardiology committee, myocardial infarction redefined—a consensus document of The Joint European Society of Cardiology/American college of cardiology committee for the redefinition of myocardial infarction, JACC 36 (2000) 959–969.
[57] <https://proteins.gelifesciences.com/products-for-proteins/spr-systems>.
[58] <https://nicoyalife.com>.
[59] B. Lee, S. Roh, J. Park, Current status of micro- and nano-structured optical fiber sensors, Opt. Fiber Technol. 15 (3) (2009) 209–221.
[60] R. Slavik, J. Homola, J. Ctyroky, Single-mode optical fiber surface plasmon resonance sensor, Sens. Actuat. B-Chem. 54 (1–2) (1999) 74–79.
[61] M. Piliarik, J. Homola, Z. Maníková, J. Čtyroký, Surface plasmon resonance sensor based on a single-mode polarization-maintaining optical fiber, Sens. Actuat. B 90 (1–3) (2003) 236–242.
[62] J. Villatoro, D. Monzon-Hernandez, E. Mejia, Fabrication and modeling of uniform-waist single-mode tapered optical fiber sensors, Appl. Opt. 42 (13) (2003) 2278–2283.

[63] Y. Wu, B.C. Yao, A.Q. Zhang, Y.J. Rao, Z.G. Wang, Y. Cheng, Y. Gong, W.L. Zhang, Y.F. Chen, K.S. Chiang, Graphene-coated microfiber Bragg grating for high-sensitivity gas sensing, Opt. Lett. 39 (5) (2014) 1235–1237.
[64] D. Li, J. Wu, P. Wu, Y. Lin, Y. Sun, R. Zhu, J. Yang, K. Xu, Affinity based glucose measurement using fiber optic surface plasmon resonance sensor with surface modification by borate polymer, Sens. Actuat. B-Chem. 213 (2015) 295–304.
[65] D. Jauregui-Vazquez, J.W. Haus, A.B. Negari, J.M. Sierra-Hernandez, K. Hansen, Bitapered fiber sensor: signal analysis, Sens. Actuat. B-Chem. 218 (2015) 105–110.
[66] A. Patnaik, K. Senthilnathan, R. Jha, Graphene-based conducting metal oxide coated D-shaped optical fiber SPR sensor, IEEE Photon. Technol. Lett. 27 (23) (2015) 2437–2440.
[67] S. Shi, L. Wang, R. Su, B. Liu, R. Huang, W. Qi, Z. He, A polydopamine-modified optical fiber SPR biosensor using electroless-plated gold films for immunoassays, Biosens. Bioelectron. 74 (2015) 454–460.
[68] L. Li, Y. Liang, Q. Liu, W. Peng, Dual-channel fiber-optic biosensor for self-compensated refractive index measurement, IEEE Photon. Technol. Lett. 28 (2016) 2110–2113.
[69] B. Lu, X. Lai, P. Zhang, H. Wu, H. Yu, D. Li, Roughened cylindrical gold layer with curve graphene coating for enhanced sensitivity of fiber SPR sensor, in: Conference on Solid-State Sensors, Actuators and Microsystems (TRANSDUCERS), 2017, http://doi.org/10.1109/TRANSDUCERS.2017.7994461.
[70] R. Kant, R. Tabassum, B.D. Gupta, Xanthine oxidase functionalized Ta_2O_5 nanostructures as a novel scaffold for highly sensitive SPR based fiber optic xanthine sensor, Biosens. Bioelectron. 99 (2018) 637–645.
[71] G. Quero, M. Consales, R. Severino, P. Vaiano, A. Boniello, A. Sandomenico, M. Ruvo, A. Borriello, L. Diodato, S. Zuppolini, M. Giordano, I.C. Nettore, C. Mazzarella, A. Colao, P.E. Macchia, F. Santorelli, A. Cutolo, A. Cusano, Long period fiber grating nano-optrode for cancer biomarker detection, Biosens. Bioelectron. 80 (2016) 590–600.
[72] T. Guo, F. Liu, B.O. Guan, J. Albert, Tilted fiber grating mechanical and biochemical sensors, Opt. Laser Technol. 78 (2016) 19–33.
[73] A. Dhawan, M.D. Gerhold, J.F. Muth, Plasmonic structures based on subwavelength apertures for chemical and biological sensing applications, IEEE Sens. J. 8 (5–6) (2008) 942–950.
[74] Y. Lin, Y. Zou, R.G. Lindquist, A reflection-based localized surface plasmon resonance fiber-optic probe for biochemical sensing, Biomed. Opt. Express 2 (3) (2011) 478–484.
[75] M. Sanders, Y.B. Lin, J.J. Wei, T. Bono, R.G. Lindquist, An enhanced LSPR fiber-optic nanoprobe for ultrasensitive detection of protein biomarkers, Biosens. Bioelectron. 61 (2014) 95–101.
[76] P.P. Jia, Z.L. Yang, J. Yang, H. Ebendorff-Heidepriem, Quasiperiodic nanohole arrays on optical fibers as plasmonic sensors: fabrication and sensitivity determination, Acs Sens. 1 (8) (2016) 1078–1083.
[77] X. Duan, L. Mu, S.D. Sawtelle, N.K. Rajan, Z.Y. Han, Y.Y. Wang, H.M. Qu, M.A. Reed, Functionalized polyelectrolytes assembling on nano-bioFETs for biosensing applications, Adv. Funct. Mater. 25 (15) (2015) 2279–2286.
[78] Z. Han, Y. Wang, X. Duan, Biofunctional polyelectrolytes assembling on biosensors – a versatile surface coating method for protein detections, Anal. Chim. Acta 964 (2017) 170–177.
[79] S. Ashkenazi, C.Y. Chao, L.J. Guo, M. O'donnell, Ultrasound detection using polymer microring optical resonator, Appl. Phys. Lett. 85 (22) (2004) 5418–5420.
[80] S.W. Huang, S.L. Chen, T. Ling, A. Maxwell, M. O'Donnell, L.J. Guo, S. Ashkenazi, Low-noise wideband ultrasound detection using polymer microring resonators, Appl. Phys. Lett. 92 (19) (2008) 193509.
[81] C. Zhang, T. Ling, S.L. Chen, L.J. Guo, Ultrabroad bandwidth and highly sensitive optical ultrasonic detector for photoacoustic imaging, ACS Photon. 1 (2014) 1093–1098.
[82] P. Morris, A. Hurrell, A. Shaw, E. Zhang, P.C. Beard, A Fabry-Pérot fiber-optic ultrasonic hydrophone for the simultaneous measurement of temperature and acoustic pressure, J. Acoust. Soc. Am. 125 (2009) 3611.
[83] T.J. Allen, E. Zhang, P.C. Beard, Large-field-of-view laser-scanning OR-PAM using a fiber optic sensor, Proc. of SPIE 93230 (2015) 932301.
[84] S.J. Mathews, E.Z. Zhang, A.E. Desjardins, P.C. Beard, Miniature fiber optic probe for minimally invasive photoacoustic sensing, Proc. SPIE 9708 (2016) 97082R.
[85] J.A. Guggenheim, E.Z. Zhang, P.C. Beard, Planoconcave optical microresonator sensors for photoacoustic imaging: pushing the limits of sensitivity (conference presentation), Proc. SPIE 9708 (2016) 97082M.
[86] T.X. Wang, R. Cao, B. Ning, A.J. Dixon, J.A. Hossack, A.L. Klibanov, Q. Zhou, A. Wang, S. Hu, All-optical photoacoustic microscopy based on plasmonic detection of broadband ultrasound, Appl. Phys. Lett. 107 (15) (2015) 153702.
[87] W. Rohringer, S. Preißer, M. Liu, S. Zotter, Z. Chen, B. Hermann, H. Sattmann, B. Fischer, W. Drexler, All-optical highly sensitive broadband ultrasound sensor without any deformable parts for photoacoustic imaging, Proc. SPIE 9708 (2016) 970815.
[88] S. Zhang, J. Chen, S. He, Novel ultrasound detector based on small slot micro-ring resonator with ultrahigh Q factor, Opt. Commun. 382 (2017) 113–118.
[89] K.H. Kim, W. Luo, C. Zhang, C. Tian, L.J. Guo, X. Wang, X. Fan, Air-coupled ultrasound detection using capillary-based optical ring resonators, Sci. Rep. 7 (2017) 109.

Tian Yang is an Associate Professor at the University of Michigan - Shanghai Jiao Tong University Joint Institute. He got the B.S. degree in Electrical Engineering from Tsinghua University in 2000, the Ph.D. degree in Electrical Engineering from the University of Southern California in 2006, took a postdoctoral fellow then research associate position at Harvard University from 2006-2009, and joined SJTU in 2009. He is the Principal Investigator of the Nanophotonics Laboratory and the Associate Director of the Center of Optics and Optoelectronics. His current research interests include fiber-optic integrated plasmonic devices and light-matter interactions in plasmonic hotspots.

Xiaolong He received his BSc (2010) in Electrical & Computer Engineering, MSc (2013) in Electrical Science & Engineering and PHD (2016) in Optical Engineering from Joint Institute, Shanghai Jiao Tong University (China) under the supervision of Prof. Tian Yang. His research focused on surface plasmon resonance device and its application for biosensing. After graduation, he started up a company (Xu Yuan Biotechnology Co. Ltd.) for providing fiber based label-free biosensing solutions for biological & medical scientific research, IVD applications et.al. Currently he is serving as CEO of the company.

Xin Zhou received the B.S. degree from the Department of Electronic Science and Engineering, Southeast University, Nanjing, China, in 2014. He is currently working toward the Ph.D. degree in University of Michigan – Shanghai Jiao Tong University Joint Institute at Shanghai Jiao Tong University. He has been engaged in research on surface plasmon resonance cavities on fiber end-facets and related biosensing and photoacoustic detection.

Zeyu Lei received his B.S. degree in optical information science and technology from Sun Yat-sen University in 2013. He is currently a Ph.D. candidate in University of Michigan-Shanghai Jiao Tong University Joint Institute. His research interests include nano-optics, metasurfaces, plasmonics, and lab-on-fiber technologies.

Yalin Wang received a Bachelor's degree in Biotechnology from Nanjing University of Science and Technology in the year of 2005 and a Doctor's degree in Microbiology from Shanghai Jiao Tong University in the year of 2011. Her research focused on in-vitro diagnosis and epidemiological investigation. She was formerly the senior biochemical researcher at Pall Fortebio LLC (2012-2014), which develops analytical systems that enable real-time analysis of biomolecular interactions. Then, she left Pall Fortebio to become a R&D Manager in Biology in Xu Yuan Biotechnology Co. Ltd. (Shanghai, China) for the development of fiber-based SPR analysis of biomolecular interactions.

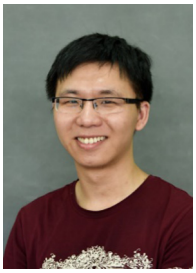

Jie Yang received his BSc (2009) from Jilin University (China), MSc (2011) from Université Lille 1 (France) and PhD in Physics (2014) from Ecole Polytechnique (France) under the supervision of Dr. Anne-Chantal Gouget-Laemmel. His research focused on Si-based surface chemistry and protein biochips. He then joined Prof. Tian Yang's group at the SJTU as a postdoctoral fellow, where he studied the chemical elaboration of SPR biosensors on optical fiber end-facets.

De Cai received the B.S. degree in Optical Information of Science & Technology at Huazhong University of Science and Technology in 2014. He joined the department of ECE of Joint Institute at Shanghai Jiao Tong University in 2014 as a graduate student. His research interest is the development of photoacoustic microscopy for disease diagnosis and monitoring.

Sung-Liang Chen is currently an Assistant Professor at the University of Michigan-Shanghai Jiao Tong University Joint Institute, Shanghai, China. He received his Ph. D. degree in electrical engineering at the University of Michigan, Ann Arbor, and postdoctoral training at the University of Michigan Medical School. His research interests include optical resonators for sensing applications, optical imaging systems, and biomedical photoacoustic imaging. He is the recipient of the Thousand Talents Plan given by the Chinese Recruitment Program of Global Experts for young professionals and Shanghai Pujiang Talent Award.

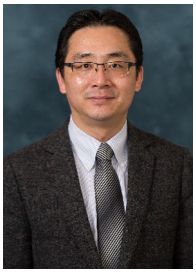

Dr. Xueding Wang is currently an Associate Professor at the Department of Biomedical Engineering, University of Michigan. Before working as an independent principle investigator, Dr. Wang received his Ph.D. at Texas A&M University and Postdoctoral training at the University of Michigan. Dr. Wang has extensive experience in development of medical imaging and treatment technologies, especially those involving light and ultrasound. Sponsored by NIH, NSF, DoD and other funding agencies, his research has led to over 100+ peer-reviewed publications. He is sitting on the editorial boards of scientific journals including Photoacoustics, Ultrasonic Imaging, and Journal of Biomedical Optics.